объединенный
институт
ядерных
исследований
дубна

E4-85-143

Dao Tien Khoa, K.V.Shitikova*

MICROSCOPIC STUDY OF ELASTIC AND INELASTIC HEAVY-ION SCATTERING

Submitted to "Nuclear Physics"

* Institute of Nuclear Physics,
Moscow State University

1985

1. INTRODUCTION

In recent years, heavy-ion (HI) scattering of projectiles of mass number $A \lesssim 30$ has already been studied with good resolution[3]. Eventhough the experimental data have been analysed rather successfully in the calculations of phenomenological models, a microscopic description of these processes is of great interest for both experimental and theoretical investigations. Such a microscopic understanding of HI collisions may be founded on the calculation of the HI interaction potential using a realistic nucleon-nucleon (N-N) interaction[1]. Note that for this purpose the folding model[2,4] has proved to be a very convenient formalism, where the potential for HI scattering is obtained by averaging an appropriate N-N interaction over the nuclear densities of two colliding ions. In such an investigation the nuclear structure information is embodied in the nuclear wave functions that determine the ground-state and transition densities, and it is possible to calculate not only diagonal but also nondiagonal matrix elements of HI interactions, so one can consider either elastic or inelastic scattering.

In the present work, within the folding model, elastic and inelastic scattering of ^{12}C ions from heavy spherical nuclei has been studied with the ground-state and transition nuclear densities calculated by the method of hyperspherical functions[5] and the quasiparticle-phonon nuclear model[9,10] for projectiles and target-nuclei, respectively. The method of hyperspherical functions (MHF) has first been applied to investigate elastic and inelastic scattering of ions with $A \lesssim 16$ in refs.[17,18], where the problem of possible excitation of the monopole resonance in these processes has been considered. Further, the folding-model calculations with nuclear densities computed by the MHF have been performed in refs.[6-8]. Within the quasiparticle-phonon nuclear model[9,10] (QPM) one can investigate a wide range of nuclear properties of the excitations in complex nuclei, including not only the low-lying excited states but also the giant multipole resonances. The nuclear wave functions calculated in the QPM have been applied to the description of various nuclear reaction processes, such as the excitation of magnetic multipole resonances in (e, e')[15] and (p, p')[19] reactions, the excitation of electric dipole states in (γ, γ') reactions[16], etc. In ref.[12] and the present paper QPM is used in the folding model to investigate HI scattering.

2. DETAILS OF CALCULATION

The description of the folding model and possible application of nuclear microscopic models in the study of HI elastic and inelastic scattering have been discussed thoroughly, for example, in refs. [1-3]. It should be noted that the knowledge of the wave functions used in the nuclear density calculation enables us to investigate nuclear structure phenomena observed in the HI scattering. Usually, in such folding calculations there are always two basic ingredients. One is the construction of nuclear ground state and transition densities within the microscopic models and the other is the choice of an appropriate effective N-N interaction between the projectile nucleons and the target nucleons. At first we give a brief description of the nuclear density calculation in the MHF and QPM.

2.1. MHF and the Projectile Densities

Within the MHF nucleon density distributions for a number of light nuclei have been calculated with the optimum fit to the basic experimental data, such as the binding energy, monopole resonance excitation energy, mean squared radius (RMS), the form factor of electron scattering [13], etc. In the K-harmonics method [5,14] the total wave function of a nucleus with A nucleons is usually expanded in terms of K-harmonics polynomials $Y_{K\gamma}(\theta_i)$

$$\Psi(1, 2, \ldots, A) = \xi^{-\frac{1}{2}(3A-4)} \sum_{K\gamma} \chi_{K\gamma}(\xi) Y_{K\gamma}(\theta_i), \tag{1}$$

where $\gamma = [f] \in LST$ [5]. The hyperspherical harmonics are eigenfunctions of the angular part of the Laplacian

$$\Delta_{\Omega_\ell} Y_{K\gamma}(\theta_i) = -K(K + \ell - 2) Y_{K\gamma}(\theta_i),$$

here K is an analogue of the angular momentum for $\ell = 3$ and is called the global moment. The system of equations for the energy and radial eigenfunctions is written as

$$\left\{\frac{d^2}{d\xi^2} - \frac{\mathcal{L}_K(\mathcal{L}_K+1)}{\xi^2} - \frac{2m}{\hbar^2}(E + W^{K\gamma}_{K\gamma}(\xi))\right\}\chi_{K\gamma}(\xi) = \frac{2m}{\hbar^2} \sum_{K'\gamma' \neq K\gamma} W^{K'\gamma'}_{K\gamma}(\xi)\chi_{K'\gamma'}(\xi), \tag{2}$$

where $\mathcal{L}_K = K + \frac{3A-6}{2}$ and $W^{K'\gamma'}_{K\gamma}(\xi)$ are the matrix elements of the N-N interaction potential [5,20]:

$$V = \sum_{i<j}^{A} V(r_{ij}), \quad V(r_{ij}) = f(r_{ij}) W_{\sigma\tau}. \tag{3}$$

With the wave functions calculated in the K-harmonics method, one can obtain the ground-state and transition densities for a considered nucleus of A nucleons [17,18]. In the present work we only consider the case of a single excitation of the nucleus-target, so the projectile is supposed to be in its ground state before and after the collision. Therefore, only the ground-state density of the nucleus-projectile of the form

$$\rho_0(r) = \frac{16\Gamma((5A-11)/2)}{\sqrt{\pi}\Gamma((5A-14)/2)} \int_r^\infty \frac{(\xi^2 - r^2)^{(5A-16)/2}}{\xi^{5A-13}} \chi_0^2(\xi)\, d\xi + \tag{4}$$

$$+ \frac{8(A-4)\Gamma((5A-11)/2)}{3\sqrt{\pi}\Gamma((5A-16)/2)} \int_r^\infty \frac{r^2(\xi^2 - r^2)^{(5A-15)/2}}{\xi^{5A-13}} \chi_0^2(\xi)\, d\xi$$

is included into the folding calculations of this work.

2.2. QPM and the Target Densities

It is well known that in the inelastic HI scattering at bombarding energies ~ 10 MeV per nucleon, usually, the low-lying states of low multipolarities are excited (for example, 2^+, 3^-, 4^+, 5^-... states of vibrational type in a spherical nucleus), so one needs to calculate within QPM, besides the ground-state density, the transition densities corresponding to such excitations in the nucleus-target. The general form of the QPM Hamiltonian is the following

$$H = H_{av} + H_{pair} + H_M + H_{SM}, \tag{5}$$

where H_{av} is the average field describing independent single-particle motions; H_{pair} describes the monopole pairing interaction between the neutrons or protons; H_M and H_{SM} are separable multipole and spin-multipole interaction terms generating the nuclear excitations. The one-phonon states with $\lambda^\pi = 1^-$, 2^+, 3^-, 4^+,... are generated by the multipole forces, whereas the one-phonon states with $\lambda^\pi = 1^+$, 2^-, 3^+,... by the spin-multipole forces. These effective forces include the isoscalar and isovector components

$$V_\lambda(\vec{r}_1, \vec{r}_2) = \frac{1}{2}(\kappa_0^{(\lambda)} + \kappa_1^{(\lambda)} \vec{\tau}_1\vec{\tau}_2) r_1^\lambda Y_{\lambda\mu}(\theta_1, \phi_1) r_2^\lambda Y_{\lambda-\mu}(\theta_2, \phi_2),$$
$$V_L^\sigma(\vec{r}_1, \vec{r}_2) = \frac{1}{2}(\kappa_0^{(\lambda L)} + \kappa_1^{(\lambda L)} \vec{\tau}_1\vec{\tau}_2) r_1^\lambda [\vec{\sigma}_1 Y_{\lambda\mu}(\theta_1, \phi_1)]_{LM} \cdot r_2^\lambda [\vec{\sigma}_2 Y_{\lambda\mu}(\theta_2, \phi_2)]_{L-M}. \tag{6}$$

The explicit form of the QPM Hamiltonian is given in refs.[9,10]. The contributions of H_M and H_{SM} to the ground-state density are negligible[9], so one has for this case

$$H_0 = H_{av} + H_{pair} = \sum_{jm\tau} E_j a^+_{jm} a_{jm} - \frac{1}{4} \sum_{jj'mm'\tau} G_\tau (-)^{j+j'-m-m'} \times \quad (7)$$

$$\times a^+_{jm} a^+_{j-m} a_{j'-m'} a_{j'm'},$$

where a^+_{jm} and a_{jm} are the nucleon creation and annihilation operators; $j \equiv (n, \ell, j)$ is the set of quantum numbers for a single-particle state with the energy E_j and the angular momentum projection m; $\tau = (n, p)$ is the isotopic index; G_n and G_p are the monopole pairing constants. In the single-particle-basis calculation, the average field is taken as a Woods-Saxon potential. The potential parameter set used in the QPM and the G_τ values are given in detail in ref.[11]. After Bogolubov's transformation

$$a_{jm} = u_j \alpha_{jm} + (-)^{j-m} v_j \alpha^+_{j-m}, \quad (8)$$

where α^+_{jm} and α_{jm} are the quasiparticle creation and annihilation operators, one can obtain the ground-state density for a heavy (spherical) nucleus in the form:

$$\rho_0(r) = \frac{1}{4\pi} \sum_j (2j+1) |R_j(r)|^2 v_j^2. \quad (9)$$

Here $R_j(r)$ is the radial part of the wave function for a single-particle state $j \equiv (n, \ell, j)$. In further calculations the nuclear densities are normalized to

$$4\pi \int \rho_0(r) r^2 dr = A, \quad (10)$$

where A is the mass number of the nucleus. Note that we have included into the ground-state-density calculation the effect of monopole pairing interaction between nucleons (7) unlike the shell model densities used in some other folding calculations[2,4]. For the calculation of the wave functions of various excited states in the nucleus-target the QPM Hamiltonian is transformed into the phonon representation. In contrast with some other microscopic models where the phonons are introduced in a phenomenological way, within QPM the structure of phonons is calculated microscopically, in the random phase approximation (RPA), and the phonons are superpositions of various two-quasiparticle excitations (see (13)). A short description of this procedure is the following: after the transformation into the space of quasiparticle and phonons[10], the QPM Hamiltonian can

be written in the form

$$H = \sum_{jm} \epsilon_j \alpha^+_{jm} \alpha_{jm} - \frac{1}{8} \sum_{\lambda i i' \tau} \frac{X^{\lambda i}_\tau + X^{\lambda i'}_\tau}{(2\lambda+1)\sqrt{\mathcal{Y}_\tau(\lambda i)\mathcal{Y}_\tau(\lambda i')}} [Q^+_{\lambda\mu i} + (-)^{\lambda-\mu} Q_{\lambda-\mu i}] \times \quad (11)$$

$$\times [(-)^{\lambda-\mu} Q^+_{\lambda-\mu i'} + Q_{\lambda\mu i'}] + H_{qph},$$

where

$$X^{\lambda i}_\tau = \sum^{\tau}_{j_1 j_2} \frac{[f^{\lambda}_{j_1 j_2} u^{(\pm)}_{j_1 j_2}]^2 \epsilon_{j_1 j_2}}{\epsilon^2_{j_1 j_2} - \omega^2_{\lambda i}},$$

$$\mathcal{Y}_{n,p}(\lambda i) = Y_{n,p}(\lambda i) + Y_{p,n}(\lambda i) \left\{ \frac{\frac{\kappa^{(\lambda)}_0 - \kappa^{(\lambda)}_1}{2\lambda+1} X^{\lambda i}_{n,p}}{1 - \frac{\kappa^{(\lambda)}_0 + \kappa^{(\lambda)}_1}{2\lambda+1} X^{\lambda i}_{p,n}} \right\}^2, \quad (12)$$

$$Y_{n,p}(\lambda i) = \frac{1}{2} \frac{\partial}{\partial\omega} X^{\lambda i}_{n,p} \Big|_{\omega = \omega_{\lambda i}}.$$

Since the magnetic excitations are not considered in this work, in (11) only the contributions from H_M in (5) are taken into account. Here $f^{\lambda}_{j_1 j_2}$ are the reduced single-particle matrix elements of multipole operator $r^\lambda Y_{\lambda\mu}(\theta, \phi)$ (see (6)) and $u^{(\pm)}_{j_1 j_2} = u_{j_1} v_{j_2} \pm u_{j_2} v_{j_1}$; ϵ_j and $\epsilon_{j_1 j_2}$ are the energies of one- and two-quasiparticle states, respectively. The energy $\omega_{\lambda i}$ of one-phonon state $Q^+_{\lambda\mu i}\Psi_0$ is obtained by solving the following RPA equation[10]

$$\frac{\kappa^{(\lambda)}_0 + \kappa^{(\lambda)}_1}{2\lambda+1} (X^{\lambda i}_n + X^{\lambda i}_p) - 4 \frac{\kappa^{(\lambda)}_0 \kappa^{(\lambda)}_1}{(2\lambda+1)^2} X^{\lambda i}_n X^{\lambda i}_p = 1, \quad (13)$$

$$Q^+_{\lambda\mu i}\Psi_0 = \sum_{jj'} \{ \psi^{\lambda i}_{jj'} [\alpha^+_{jm} \alpha^+_{j'm'}]_{\lambda\mu} - (-)^{\lambda-\mu} \phi^{\lambda i}_{jj'} [\alpha_{j'm'} \alpha_{jm}]_{\lambda-\mu} \} \Psi_0,$$

where Ψ_0 is the phonon vacuum. In the one-phonon approximation, i.e., in the RPA, the contribution from H_{qph} which describes the quasiparticle-phonon interaction[9,10] is absent, and one has for an excited state in the nucleus-target: $|\lambda^\pi_i> = Q^+_{\lambda\mu i}\Psi_0$.

Further, if we define the nuclear transition density as $\rho(r) = \langle f | \sum_k \delta(r - r_k) | i \rangle$ with the multipole expansion of the form

$$\rho(r) = \sum_{\lambda\mu} C_\lambda \langle J_i M_i \lambda\mu | J_f M_f \rangle \rho_\lambda(r) Y^*_{\lambda\mu}(\theta, \phi), \quad (14)$$

where the normalization constant C_λ is that defined in ref.[2], we get

$$\rho_\lambda(r) = \langle J_f \| \sum_k r_k^{-2} \delta(r - r_k) i^\lambda Y_\lambda(\theta_k, \phi_k) \| J_i \rangle . \quad (15)$$

Here the reduced matrix element (15) is as defined by Brink and Satchler [21]. In the case of single excitation of an even-even nucleus target ($J_f = \lambda$ and $J_i = 0$), after some transformations one obtains

$$\rho_\lambda(r) = \frac{1}{\sqrt{4\pi}} \sum_{j_1 \geq j_2} \frac{i^{\ell_2+\lambda-\ell_1} (-)^{j_2+\lambda+3/2}}{2(1+\delta_{j_1 j_2})} \hat{j}_1 \hat{j}_2 \begin{pmatrix} j_1 & j_2 & \lambda \\ \frac{1}{2} & -\frac{1}{2} & 0 \end{pmatrix} \times \quad (16)$$

$$\times R^*_{j_1}(r) R_{j_2}(r) u^{(+)}_{j_1 j_2} (\psi^{\lambda_i}_{j_1 j_2} + \phi^{\lambda_i}_{j_1 j_2}) [1 + (-)^{\ell_2 - \ell_1 + \lambda}].$$

It should be noted that in some other folding calculations, for example in ref.[22] preference has been given to the macroscopic Tassie model[23] in the nuclear transition density calculation. Since it is just the tails of the transition densities, which contribute most to the folding integral for the potential near the strong absorption radius (17); and those microscopic models which use an oscillator basis do not give the densities accurate enough for such large distances. In the QPM, the single-particle basis is calculated by a numerical method[24] using the code REDMEL[25], and the calculated radial wave functions describe nuclear asymptotics correctly, so the nuclear transition densities calculated within QPM are quite adequate for the use in the folding model.

2.3. HI Interaction Potential

There are various types of the effective N-N interaction which can be used in the folding calculations. For example, in ref.[8] the zero-range Skyrme forces[26] and finite-range forces in the Gaussian form[27] have been used to describe elastic scattering $^{16}O + ^{16}O$ at different bombarding energies. In the present work we have chosen the so-called M3Y effective N-N interaction[28] based upon a realistic G-matrix. In recent years the M3Y interaction is quite successfully applied in the folding model to describe elastic and inelastic HI scattering (see, for example, refs.[3,4]). Our earlier calculations[12] have also indicated that the M3Y interaction is more appropriate for the description of elastic HI scattering in comparison with the δ-Skyrme forces. The HI scattering is characterized

by the strong absorption[1,2] and most of the available data is sensitive only to the tail of the HI potential in the vicinity of some strong absorption radius

$$R_{crit} \sim 1.5(A_1^{1/3} + A_2^{1/3}) \text{ (fm)}, \quad (17)$$

In such an approximation the double-folded potential may be written as

$$U_F(\vec{R}) = \int d\vec{r}_1 d\vec{r}_2 \rho_1(\vec{r}_1) \rho_2(\vec{r}_2) v(\vec{r}_{12} = \vec{R} + \vec{r}_2 - \vec{r}_1), \quad (18)$$

where ρ_1 and ρ_2 are the nucleon densities in the nuclei A_1 and A_2, respectively; $v(\vec{r}_{12})$, the effective N-N interaction between nucleons in A_1 and nucleons in A_2. The calculation of six-dimensional integral (18) is very complicated in the coordinate space, but if we work in momentum space, this integral is reduced to a product of three one-dimensional integrals[2]. With the multipole expansion (14) one obtains, in the case of single excitation of a spin-zero target, the following expression for double-folded potential (18)

$$U_F(\vec{R}) = C_\lambda U_\lambda(R) Y^*_{\lambda\mu}(\theta_R, \phi_R),$$

where

$$U_\lambda(R) = \frac{1}{2\pi^2} \int dk\, k^2 j_\lambda(kR) \tilde{v}(k) \tilde{\rho}^{(1)}_\lambda(k) \tilde{\rho}^{(2)}_0(k), \quad (19)$$

and

$$\tilde{f}_\lambda(k) = 4\pi \int r^2 dr\, j_\lambda(kr) f_\lambda(kr). \quad (20)$$

The M3Y interaction[1,2] is

$$v(t) = 7999 \frac{\exp(-4r)}{4r} - 2134 \frac{\exp(-2.5r)}{2.5r} - 262\,\delta(r_{12}). \quad (21)$$

The inclusion of an explicit energy and density dependence into (21) generally leads to a better consistency of the calculational results with the experimental data (see ref.[29]). The elastic scattering corresponds to $\lambda = 0$ in these formulae. Further, $U_\lambda(R)$ is taken as a real part of the HI potential into the cross-section calculation. The imaginary part of the HI potential is included phenomenologically so as to fit the data for elastic cross-section. Usually[1,2], the imaginary optical potential is supposed to have a Woods-Saxon form

$$W(r) = -\frac{W_V}{1 + \exp[(r - R_V)/a_V]}, \qquad (22)$$

where $R_V = r_V(A_1^{1/3} + A_2^{1/3})$. W_V and r_V, a_V are defined from the best fit to the elastic scattering data. In this case the imaginary transition potential is defined by deforming the Woods-Saxon potential (22), i.e.,

$$W_\lambda(r) = -\beta_\lambda^I R_V \frac{dW(r)}{dr}. \qquad (23)$$

The deformation parameter β_λ^I is obtained from the B(E λ) values scaled according to $\beta R = \text{const}$ [12]. In some cases considered in this work, for the sake of simplicity, the imaginary part of the HI potential is supposed to have the same shape as the real part (in both elastic and inelastic channels). In such a simple approximation calculations have been performed with one adjustable parameter a equal to the ratio of the imaginary and real amplitudes of the HI optical potential.

2.4. Coulomb Interaction

HI reactions are characterized by the strong Coulomb interaction between the two ions. The Coulomb field plays an important role in the excitation of low-lying nuclear states, especially, the electric states of low multipolarities [1-3]. In the elastic channel the Coulomb term of the HI potential to a good approximation [1,2] may be treated as a simple Coulomb interaction between two charged spheres [2]. Note that in some applications of the folding model to the inelastic HI scattering the Coulomb excitation form factor is phenomenologically included into the calculation from the collective model with the charge deformation parameter extracted from the analysis of the measured cross-sections. In the present work the Coulomb term of the HI transition potential is calculated microscopically by the same folding formulae as for the nuclear part (18), only instead of nuclear transition densities and the M3Y interaction in these formulae stand the charge transition densities and the Coulomb interaction between two protons, respectively. The charge ground-state densities of the two ions are the proton parts of (4) and (9). The charge transition density of the nucleus-target is calculated by formula (16). In the calculation of phonon amplitude $\psi^{\lambda i}_{j_1 j_2}$ and $\psi^{\lambda i}_{j_1 j_2}$ (see (13)) the isoscalar and isovector constants of effective multipole forces $\kappa_0^{(\lambda)}$ and $\kappa_1^{(\lambda)}$ (6) have been chosen so as to satisfy the following relation

$$B_{exp}(E\lambda; O^+_{g.s.} \to \lambda^\pi) = (2\lambda + 1) \left| \int_0^\infty r^{\lambda+2} dr [e_n^{(\lambda)} \rho_{n,\lambda}(r) + e_p^{(\lambda)} \rho_{p,\lambda}(r)] \right|^2, \qquad (24)$$

where $B_{exp}(E\lambda)$ is the measured transition probabilities for the lowest excited state with spin λ and parity π; $\rho_{n,\lambda}(r)$ and $\rho_{p,\lambda}(r)$ the neutron and proton parts of (16); $e_n^{(\lambda)}$ and $e_p^{(\lambda)}$ the effective neutron and proton charges in the nucleus [10] (for states with $\lambda \geq 2$ $e_n^{(\lambda)} = 0$ and $e_p^{(\lambda)} = e$).

3. RESULTS OF CALCULATION AND SOME DISCUSSIONS

The transition folded potential $U_\lambda(R)$ (19) must, generally, be used in the coupled channel calculations for the description of inelastic HI scattering. However, as it has been shown in other folding calculations [1,2], a qualitative agreement with the experimental data can be reached in the distorted-wave Born approximation (DWBA), especially, in the description of the lowest 2+, 3− excited states in the nucleus-target, which have a strong one-phonon structure [3,9,10]. In the present work all calculations have been performed within the DWBA using a modified version of the code DWUCK [30]. The imaginary potential parameters have been defined from the best fit to the elastic data using an optical model program with the search package MINUIT [31]. The phonon amplitudes ψ and ϕ have been calculated by the code RPAS [32] which performs the RPA calculations within QPM.

In this work we consider elastic and inelastic scattering of ^{12}C ions from some heavy spherical nuclei at different bombarding energies. The nuclear ground-state density for ^{12}C has been calculated in the MHF with the N-N potential V7 [20]. This calculation gives the mean squared radius RMS = 2.325 fm, the binding energy E_b =83.1 MeV and minimum in the form factor of elastic electron scattering [13] q = 4.1 fm^{-1} compared to the experimental data (RMS (exp.) = 2.294 fm, E_b (exp.) = 92.2 MeV and q (exp.) = 4.1 fm^{-1}) for ^{12}C nucleus. The structure of the low-lying excited states in the nuclei-targets has been calculated with the sets of constants $(\kappa_0^{(\lambda)}, \kappa_1^{(\lambda)})$ which reproduce the excitation energies and the reduced transition probabilities shown in the table.

In the description of various excitations in the nucleus-target, from the point of view of QPM, it is important to know how $(\kappa_0^{(\lambda)}, \kappa_1^{(\lambda)})$ influence the calculated inelastic cross-sections. Theoretical study of the same nuclear states excited in different reactions enables us to choose the most appropriate set of $(\kappa_0^{(\lambda)}, \kappa_1^{(\lambda)})$ for the calculation of the wave functions of excited states with spin λ and parity π (see the table). The results of the microscopic DWBA calculation for

Table

The structure of the low-lying excited states in the nuclei-targets calculated in the RPA

Target	λ^π	$\omega_{\lambda\pi}$ (MeV) expt.	$\omega_{\lambda\pi}$ (MeV) calc.	$B(E\lambda\uparrow)$ (e^2b^λ) expt.	$B(E\lambda\uparrow)$ (e^2b^λ) calc.	RMS(fm)
^{90}Zr	2^+	2.19	2.63	0.06 , 0.072	0.074	
	3^-	2.75	2.72	0.074 , 0.108	0.071	4.313
^{142}Nd	2^+	1.57	1.75	0.34 , 0.47	0.348	
	3^-	2.08	2.07	0.24	0.22	4.932
^{144}Nd	2^+	0.696	1.15	0.40 , 0.51	0.479	
	3^-	1.51	1.81	0.26	0.282	4.946
^{208}Pb	2^+	4.086	4.64	0.30 ± 0.02	0.301	
	3^-	2.61	2.64	0.69 ± 0.05	0.695	5.588
	5^-	3.194	3.2	0.046±0.006	0.054	

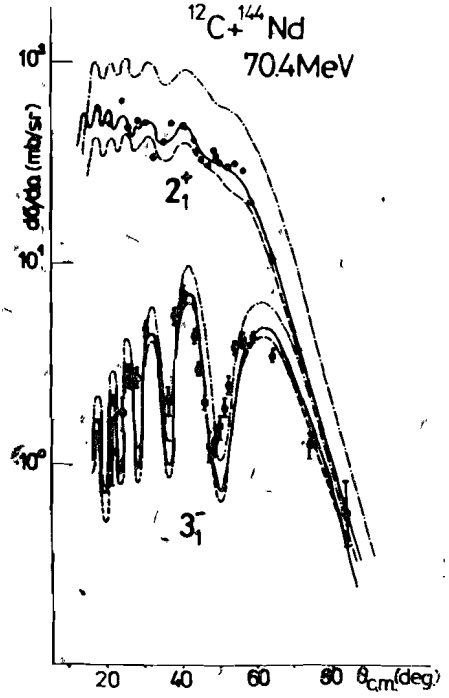

Fig.1. The inelastic cross-sections for $^{12}C + ^{144}Nd$ at 70.4 MeV calculated with different sets of isoscalar and isovector constants (see details in Sec.3).

$^{12}C + ^{144}Nd$ at 70.4 MeV /33/ with different sets of $(\kappa_0^{(\lambda)}, \kappa_1^{(\lambda)})$ are shown in fig.1. The dash-dotted curves correspond to the κ_0 and κ_1 which generate the lowest 2^+ and 3^- one-phonon states with the energies $\omega_{2_1^+}$ = = 0.696 MeV, $\omega_{3_1^+}$ = 1.51 MeV and the reduced transition probabilities $B(E2; 0^+ \to 2_1^+)$ = = 0.975 e^2b^2, $B(E3; 0^+ \to 3_1^-)$ = = 0.382 e^2b^3 respectively. The dashed curves correspond to

$\omega_{2_1^+}$ = 1.25 MeV, $\omega_{3_1^-}$ = 1.9 MeV and $B(E2\uparrow)$ = 0.411 e^2b^2, $B(E3\uparrow)$ = = 0.257 e^2b^3; and the solid curves $\omega_{2_1^+}$ = 1.15 MeV, $\omega_{3_1^-}$ = 1.81 MeV and $B(E2\uparrow)$ = 0.479 e^2b^2, $B(E3\uparrow)$ = 0.282 e^2b^3. From various compilations of the experimental data /33,34/ for nucleus ^{144}Nd one has $\omega_{2_1^+}$ (exp.) = 0.696 MeV, $\omega_{3_1^-}$ (exp.) = 1.151 MeV and $B(E2\uparrow)_{exp}$ = = 0.40 e^2b^2, 0.51 e^2b^2; $B(E3\uparrow)$ = 0.26 e^2b^3. As one can see, good agreement of the calculated cross-sections with inelastic data is provided by the sets of constants $(\kappa_0^{(\lambda)}; \kappa_1^{(\lambda)})$ giving the calculated $B(E\lambda)$-values close to the measured ones, but the calculated excitation energies $\omega_{\lambda\pi}$ are somewhat higher than the experimental data (see also the Table). Numerous calculations within QPM /10,35/ have shown that good agreement with the data for both the excitation energy and $B(E\lambda)$-value can be reached by including into the nuclear wave function more complicated two-phonon components which allow for anharmonic effects in the collective excitation.

The effects of interference between the Coulomb and nuclear excitations are of special interest, because the form of the Coulomb interaction is known and the information about the nuclear interaction may be obtained by extracting accurately the relative phase between the Coulomb and nuclear contributions to the inelastic data /1,3,36/. We have considered these effects on the same example of $^{12}C + ^{144}Nd$ at 70.4 MeV. As one can see from Fig.2 and upper part of fig.3, the contribution from the Coulomb part of the HI transition folded potential is dominant in the case of 2_1^+ excitation in ^{144}Nd-target, whereas the nuclear and Coulomb parts are comparable (see the lower part of Fig.3) for the 3_1^- excitation. Our calculation has shown that the interference in this case reverses the phase of the oscillations at forward angles. This is consistent with the experimental-data analysis performed in ref. /33/ using the phenomenological collective model.

Further we consider the elastic and inelastic ^{12}C scattering on ^{208}Pb at 98 MeV and 116.4 MeV, ^{90}Zr at 98 MeV and Nd isotopes at 70.4 MeV /33,37-39/. On the whole, our calculation gives a good description for these data (see figs.4,5), the only exception is the case of 2^+ excitation in ^{208}Pb induced by ion ^{12}C at 98 MeV when the calculated inelastic cross-section underestimates the data by a factor of about two (see fig.4b). This fact is not understandable within the folding model /38/. The calculated elastic cross-sections shown in fig.4a for system $^{12}C + ^{208}Pb$ at bombarding energies 96 MeV and 116.4 MeV /37/ point to some advantage of the nuclear ground-state densities used in this work compared to the shell model densities used in some other folding calculations /2/. (It is impossible to fill the observed maxima in the elastic cross-sections with the shell model densi-

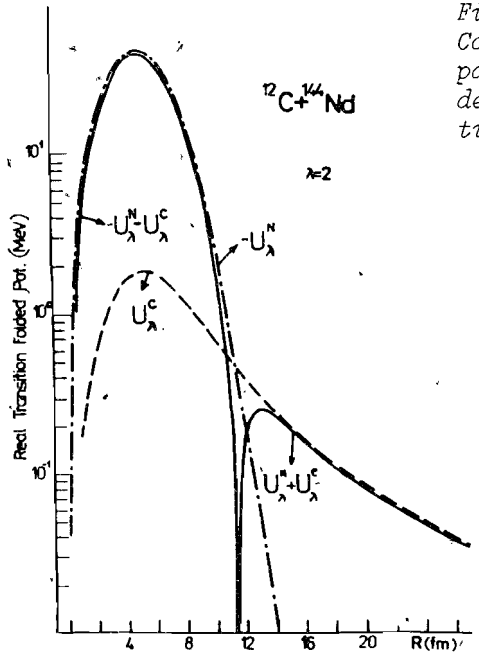

Fig.2. The contributions from Coulomb U_λ^C and nuclear U_λ^N parts to the HI transition folded potential for the, 2_1^+ excitation in ^{144}Nd induced by ^{12}C ion.

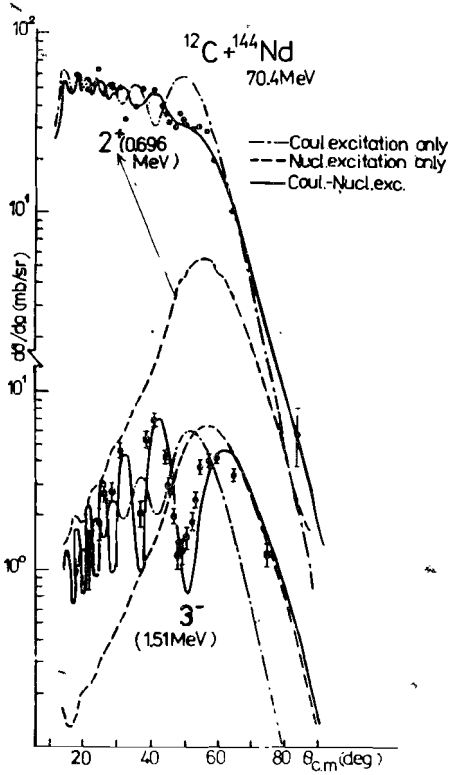

Fig.3. The interference between Coulomb and nuclear interactions in the case of 2_1^+ and 3_1^- excitations in ^{144}Nd.

ties not renormalizing the strength of the interaction - the dashed lines in fig.4a).

4. CONCLUSION

The microscopic nuclear models (the method of hyperspherical functions and quasiparticle-phonon nuclear model) are applied to study the elastic and inelastic heavy-ion scattering within the framework of the folding model. Results of our calculations reproduce the experimental data in most considered cases and this indicates the validity of further application of the MHF and QPM to the HI scattering.

The influence of the microscopic structure of the wave functions for considered nuclei on the calculated cross-sections is discussed. Theoretical investigation of the interference between the Coulomb and nuclear excitations using microscopic charge and nuclear densities gives results consistent with the phenomenological analysis of these processes.

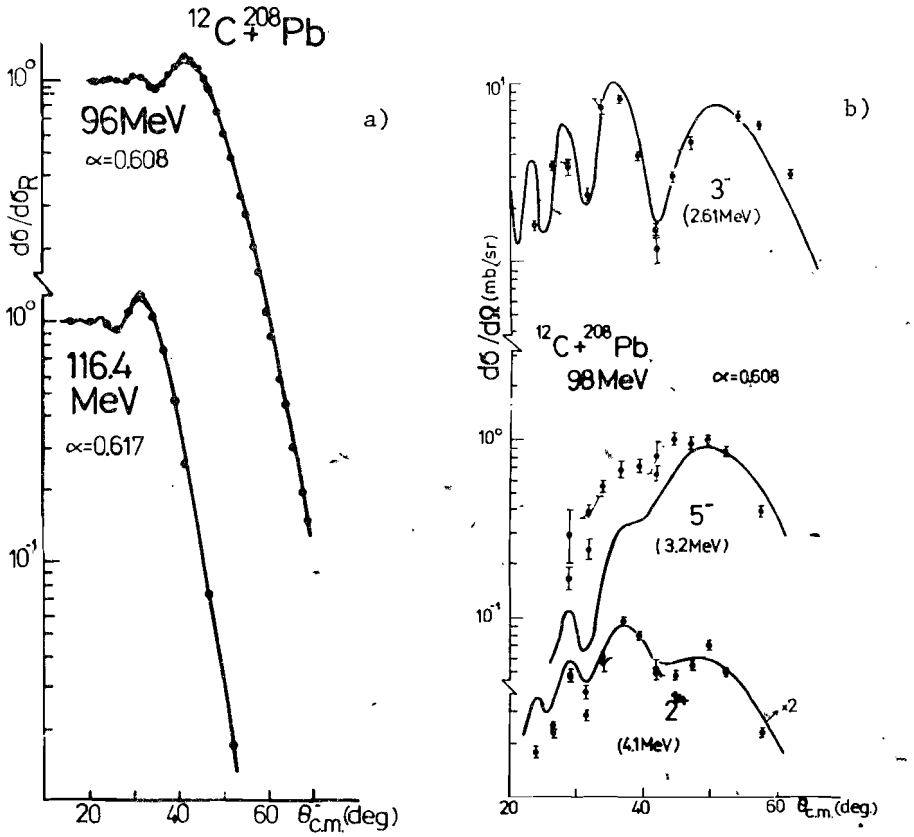

Fig.4. The calculated elastic and inelastic cross-sections of ^{12}C scattering on ^{208}Pb.

The authors are indebted to prof. V.G.Soloviev and F.A.Gareev for useful discussions, A.I.Vdovin for some critical remarks. We also thank S.N.Ershov, N.Yu.Shirikova and Yu.I.Shelontsev for help in the numerical calculations.

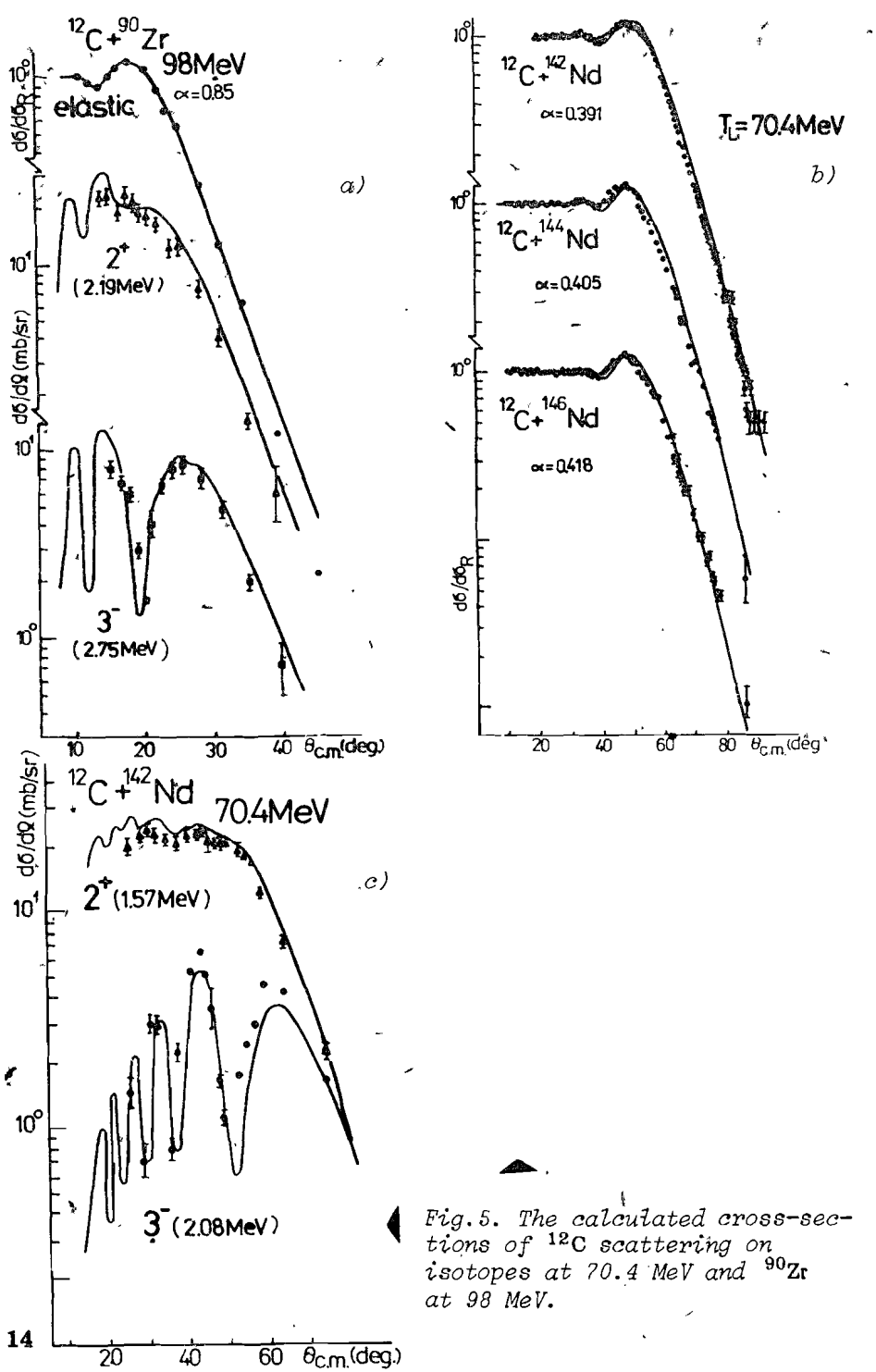

Fig.5. The calculated cross-sections of ^{12}C scattering on isotopes at 70.4 MeV and ^{90}Zr at 98 MeV.

REFERENCES

1. Satchler G.R. Direct Nuclear Reactions, Oxford University Press, Oxford, 1983.
2. Satchler G.R., Love W.G. Phys.Rep., 1979, vol.55, p.183.
3. Broglia R.A., Winther A. Heavy Ion Reactions: Lecture Notes, Addison-Wesley, Reading, Massachusetts, 1981, vol.I.
4. Satchler G.R. Nucl.Phys., 1979, A329, p.233.
5. Shitikova K.V. Nucl.Phys., 1979, A331, p.365.
6. Dëmyanova A.S., Shitikova K.V. Yad.Fiz., 1982, vol.35, p.1431.
7. Burov V.V. et al. Z.Phys., 1983, A313, p.319.
8. Nazmitdinov R.G., Saupe G., Shitikova K.V. Yad.Fiz., 1984, vol.39, p.1415.
9. Soloviev V.G. Theory of Complex Nuclei, Pergamon Press, Oxford, 1976; Soloviev V.G. Particles and Nuclei, 1978, vol.9, p.580.
10. Vdovin A.I., Soloviev V.G. Particles and Nuclei, 1983, vol.14, p.237; Voronov V.V., Soloviev V.G. ibid., 1983, vol.14, p.1381.
11. Ponomarev V.Yu. et al. Nucl.Phys., 1979, A323, p.446.
12. Dao Tien Khoa, Shitikova K.V. JINR, E4-84-305, Dubna, 1984.
13. Kashiev M., Shitikova K.V. Yad.Fiz., 1979, vol.30, p.1479; Burov V.V. et al. J.Phys.G: Nucl.Phys., 1981, vol.7, p.137.
14. Smirnov Yu.F., Shitikova K.V. Particles and Nuclei, 1977, vol.8, p.847.
15. Vdovin A.I., Ponomarev V.Yu., Shilov V.M. Yad.Fiz., 1981, vol.34, p.1009.
16. Voronov V.V., Dao Tien Khoa, Ponomarev V.Yu. Izv.Akad.Nauk SSSR (ser.fiz.), 1984, vol.48, p.1846; Voronov V.V., Dao Tien Khoa, ibid., 1984, vol.48, p.2008.
17. Dymarz R., Shitikova K.V. JINR, E7-81-653, Dubna, 1981.
18. Dymarz R., Molina J.I., Shitikova K.V. Z.Phys., 1981, A299, p.245.
19. Ponomarev V.Yu. et al. JINR, E4-83-497, Dubna, 1983.
20. Brink D.M., Boeker E. Nucl.Phys., 1967, A91, p.1.
21. Brink D.M., Satchler G.R. Angular Momentum, Oxford University Press, Oxford, 1971.
22. Bertrand F.E. et al. Phys.Rev., 1980, C22, p.1832.
23. Tassie L.J. Austral.J.Phys., 1956, vol.9, p.407; Mackintosh R.S., Tassie L.J. Nucl.Phys., 1974, A222, p.187.
24. Bang J. et al. Nucl.Phys., 1976, A261, p.59.
25. Gizatkoulov M.Kh. et al. JINR, P11-10029, Dubna, 1976.
26. Vautherin D., Brink D.M. Phys.Lett., 1970, 32B, p.149.
27. Knyazkov O.M., Haftor E.F. Z.Phys., 1981, A301, p.277.
28. Bertsch G. et al. Nucl.Phys., 1977, A284, p.399.

29. Kobos A.M. et al. Nucl.Phys., 1982, A384, p.65.
30. Kunz P.D. University of Colorado, unpublished.
31. James F., Roos M. Comp.Phys.Comm., 1975, vol.10, p.393.
31. Stoyanov Ch., Yudin I.P. JINR, P4-11076, Dubna, 1977.
32. Hillis D.L. et al. Phys.Rev., 1977, C16, p.1467.
34. Nuclear Data Sheets, 1979, vol.27, p.126.
35. Vdovin A.I., Stoyanov Ch. Izv.Akad.Nauk SSSR (ser.fiz.), 1973, vol.37, p.1750.
36. Christensen P.R. et al. Nucl.Phys., 1973, A207, p.433.
37. Ball J.B. et al. Nucl.Phys., 1975, A252, p.208.
38. Satchler G.R. et al. Phys.Lett., 1975, 60B, p.43.
39. Thorton S.T. et al. Phys.Rev., 1976, C13, p.1502.

Received by Publishing Department
on February 27, 1985.

Дао Тиен Кхоа, Шитикова К.В. E4-85-143

Микроскопическое изучение упругого
и неупругого рассеяния тяжелых ионов

Метод гиперсферических функций и квазичастично-фононная модель применяются для микроскопического изучения упругого и неупругого рассеяния тяжелых ионов. Потенциал взаимодействия тяжелых ионов рассчитывается в рамках фолдинг-модели с эффективным M3Y нуклон-нуклонным взаимодействием. Обсуждаются интерференция между кулоновским и ядерным взаимодействиями и проявление микроскопической структуры волновых функций ядер в исследуемых реакциях.

Работа выполнена в Лаборатории теоретической физики ОИЯИ.

Препринт Объединенного института ядерных исследований. Дубна 1985

Dao Tien Khoa, Shitikova K.V. E4-85-143

Microscopic Study of Elastic
and Inelastic Heavy-Ion Scattering

The method of hyperspherical functions and the quasiparticle-phonon nuclear model are applied for microscopic study of elastic and inelastic heavy ion scattering. The heavy-ion interaction potential is calculated within the folding-model using the M3Y effective nucleon-nucleon interaction. Contributions from the nuclear and Coulomb parts of the heavy-ion potential to the excitation of low-lying one-phonon states in nuclei-target and the influence of isoscalar and isovector effective forces used in the phonon calculation have been considered. Some effects of the microscopic nuclear wave functions used in the density calculation are also indicated.

The investigation has been performed at the Laboratory of Theoretical Physics, JINR.

Preprint of the Joint Institute for Nuclear Research. Dubna 1985